Interactions of Oxygen and Hydrogen on Pd(111) surface

D. O. Demchenko[1], G. M. Sacha[2], M. Salmeron[2] and L.-W. Wang[1]
[1] *Computational Research Divisions, Lawrence Berkeley National Laboratory, Berkeley CA 94720*
[2] *Materials Science Divisions, Lawrence Berkeley National Laboratory, Berkeley CA 94720*

ABSTRACT

The coadsorption and interactions of oxygen and hydrogen on Pd(111) was studied by scanning tunneling microscopy and density functional theory calculations. In the absence of hydrogen oxygen forms a (2×2) ordered structure. Coadsorption of hydrogen leads to a structural transformation from the (2×2) to a (√3×√3)R30° structure. In addition to this transformation, hydrogen enhances the mobility of oxygen. To explain these observations, the interaction of oxygen and hydrogen on Pd(111) was studied within the density functional theory. In agreement with the experiment the calculations find a total energy minimum for the oxygen (2×2) structure. The interaction between H and O atoms was found to be repulsive and short ranged, leading to a compression of the O islands from (2×2) to (√3×√3)R30° ordered structure at high H coverage. The computed energy barriers for the oxygen diffusion were found to be reduced due to the coadsorption of hydrogen, in agreement with the experimentally observed enhancement of oxygen mobility. The calculations also support the finding that at low temperatures the water formation reaction does not occur on Pd(111).

Keywords: Oxygen, hydrogen, palladium, density functional theory, *ab initio* calculations, scanning tunneling microscopy.

1. INTRODUCTION

The study of the interaction forces between coadsorbed species is important for a fundamental understanding of chemical processes on surfaces in heterogeneous catalysis. Coadsorbed species can interact not only by simple site blocking and exclusion, but also via substrate-mediated interactions, where atoms of one species induce the rearrangement of nearby substrate atoms and/or affect their electronic structure, which in turn influences the adsorption of other species [1].

The coadsorption of hydrogen and oxygen is a textbook case, being the first step in the catalytic formation of water [2,3,4,5,6,7,8,9]. Oxygen molecules adsorb intact on the Pd(111) surface forming ordered (2×2) islands at low temperature but when the temperature is increased to 120 K thermal dissociation can be observed to occur on the time scale of minutes, and at 160 K all the molecules have dissociated, forming a (2×2) ordered phase [10,11].

Molecular hydrogen dissociates readily upon adsorption at 40 K. At saturation, dissociated hydrogen forms a (1×1) ordered phase on the Pd(111) surface occupying the fcc sites, as shown both experimentally [12] and theoretically [13]. Ordered (√3×√3)R30° phases have also been reported [14]. According to low energy electron diffraction (LEED) studies and theoretical calculations, the preferential adsorption site for both atoms is the threefold hollow site on the fcc (111) surface [15,16,17,18,19].

We have studied the structures formed by atomic hydrogen as a function of coverage and its diffusion behavior on Pd(111) using STM [20,21]. As the coverage increases, isolated atoms coalesce first into (√3×√3)R30° islands with local coverage of 0.33, followed by another (√3×√3)R30° phase with coverage 0.66. At higher coverage (1×1) phase is formed.

When coadsorbed with CO, a transformation of the atomic oxygen structure from (2×2) to (√3×√3)R30° was reported to occur at 200 K by LEED. It was suggested that the transformation was due to coadsorption of residual hydrogen or CO in the vacuum system [22]. A similar (2×2) → (√3×√3)R30° transformation was observed in our experiments upon addition of hydrogen above 150 K [23]. Interestingly, the two species

remained separated in different domains up to 210 K, at which point the surface H atoms diffused into the bulk causing the reverse $(\sqrt{3}\times\sqrt{3})R30^{o} \rightarrow (2\times2)$ transformation without loss of oxygen atoms. Only above 220 K and in the presence of gas phase H_2 did the coverage of O decrease by reaction with H to form water. In addition, the study showed an increase in O ad-atom mobility due to the presence of H atoms.

In this paper we present Density Functional Theory (DFT) calculations of the energetics of the O-H interaction that help understand the reported transformations as well as the enhanced diffusivity of oxygen described above. In addition several new results on the evolution of the O structures due to coadsorption with H are presented that expand our knowledge of this interesting O-H system. We found that the (2×2)-O structure is indeed the lowest energy configuration for coverages below 0.25, although the calculated energy difference with other O structures is quite small. We show that the coadsorption of hydrogen produces the energy necessary to compress oxygen into the less stable $(\sqrt{3}\times\sqrt{3})$-O structure. We also show that the mobility of O atoms and the repulsion between H and O are closely related.

2. EXPERIMENTAL AND THEORETICAL METHODS

2.1 Experimental

The details of the experimental set-up were presented in previous publications (Refs. 20,21,23), and therefore only a brief description is given here. A home made scanning tunneling microscope was used in an ultrahigh vacuum (UHV) chamber with background pressure below 2×10^{-10} Torr. The sample temperature could be varied between 35 K and room temperature. The sample was prepared by several cycles of noble gas bombardment at 1000 K with subsequent flashing to 1100 K. This procedure generated a clean, well-ordered surface.

Surfaces with submonolayer coverage of atomic O were prepared by exposing the samples to 1.5 Langmuir of oxygen followed by annealing to 260 K for 10s. Molecular dissociation was observed above 130 K, with the atomic oxygen diffusing and forming (2×2)-O islands. In addition to the (2×2)-O islands, lines of O atoms were also observed to form. Hydrogen was adsorbed by exposure to the gas phase at 35 K, introduced into the chamber using a variable leak valve.

2.2 Theoretical

All geometry optimizations and total energy calculations were performed using the VASP code [24,25]. The Kohn-Sham equations of the DFT were solved within the generalized gradient approximation (GGA) of Perdew and Wang [26,27]. Since the adsorption energy difference among possible oxygen structures on the surface is rather small (tens of meV per oxygen atom), careful convergence tests were performed to ensure reliable total energy differences and geometries [28]. For the Brillouin zone integration a 8×8×1 Monkhorst-Pack **k**-points grid was used for the unit cell containing a (111) surface. Plane wave basis sets with a kinetic energy cutoff of 400 eV were found sufficient to ensure reliable total energy error cancellation between the oxygen covered and the bare surface. In most cases the structure relaxation was preformed using conjugate gradient and DIIS algorithms [29] until the forces on the atoms were reduced to 0.005 eV/Å or less. The lattice constant of bulk fcc Pd was found to be a = 3.95 Å, a value that was used in all subsequent calculations. The larger lattice constant of Pd in the GGA was previously reported to lead to ferromagnetic solutions, contrary to the experiment, where bulk Pd is found to be paramagnetic. Here we also find that the bare Pd(111) surface is ferromagnetic, with the energy of the ferromagnetic phase lower than that of the non-magnetic phase by 3.83 meV/atom, and with local magnetic moments varying from 0.28 μ_B/atom in the surface layer to 0.42 μ_B/atom in the bulk-like layers. However, in the presence of oxygen the calculated local magnetic moments of oxygen atoms were found to vanish. In addition, the adsorption

energies of the (2×2)-O and (4×4)-O structures were higher in the magnetic calculations by 47.9 and 70.5 meV/(O atom), respectively. Hence, in most calculations spinless electrons were considered. On one hand, this will not alter the results for local magnetic moment of the O atoms. On the other hand, it will align with the experimental bulk Pd magnetic moment. Based on our tests even if spin is included in our calculations, the results do not change appreciably.

The surfaces were represented by periodic slabs, separated by vacuum layers equivalent to at least 4 Pd monolayers. The surface unit cell used in the calculations contains 16 primitive Pd unit cells. The Pd atoms in the bottom layer were kept fixed, while all other Pd, oxygen, and hydrogen atoms on the surface were allowed to relax.

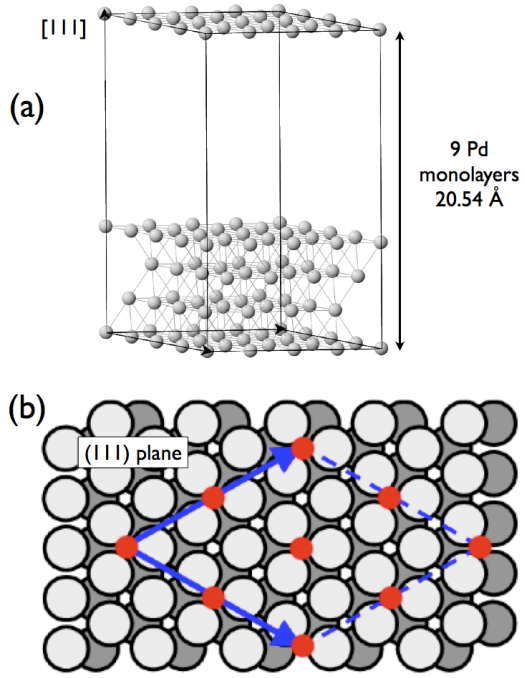

Figure 1. (a) Supercell used in the calculations. Four layers of Pd are stacked in (111) direction and separated by 13.7 Å of vacuum; (b) (2×2) oxygen (red circles) structure on Pd(111) with each oxygen occupying every other fcc hollow site on the surface.

The unit cell used in the calculations is shown in Figure 1(a). Four palladium layers are stacked along the *z* axis (fcc (111) axis), with the length of the supercell equal to 9 Pd layers. In total, there are 64 Pd atoms in the supercell. Due to the different symmetry in cases of the (3×3)-O, (√3×√3)-3O, and (√3×√3)-O structures, we used a supercell containing 9 primitive Pd unit cells on the surface, with the same Pd slab thickness and vacuum spacing.

3. RESULTS AND DISCUSSION

3.1 Experimental results

After dissociation of the adsorbed O_2 by heating to 260 K, islands of O with (2×2) periodicity were observed. Other arrangements of O atoms were also observed, including isolated atoms and lines of atoms separated by distances 2 and √3 times the Pd lattice, following the principal crystallographic directions of the substrate. Examples of these structures are shown in the STM images of Figure 2. In the images O appears as a depression, about 0.4 Å when isolated, a well know electronic effect due to the loss of density of states at the Fermi edge near the oxygen atoms [30]. The broad brighter spots in the figure between the O structures correspond to ~ 0.1 Å protrusions due to subsurface impurities. They have been described in detail previously [31].

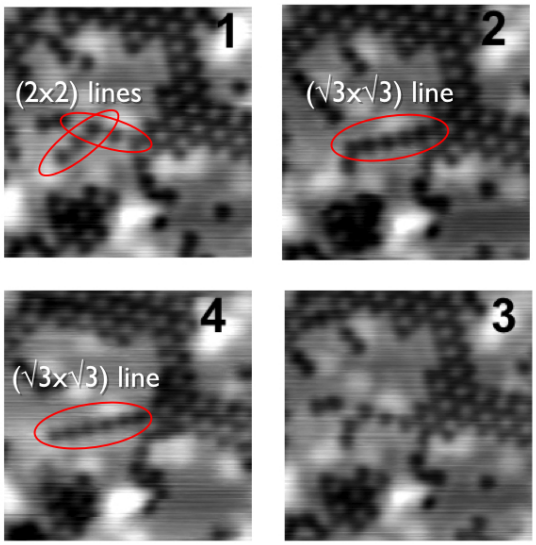

Figure 2. STM images at 144 K, showing (2×2) oxygen islands, isolated atoms and lines of atoms separated by 2 and √3 times the Pd-Pd distance. The O atoms appear as dark spots. Introduction of H (between the first and second image) results in an enhanced mobility of the O atoms, as shown in this sequence of images (1/min). The H atoms are not visible in these images due to their weak

contrast (<5 pm) and high mobility. The broad high intensity (white) patches are due to subsurface impurities.

The isolated oxygen atoms are immobile below 160 K, but hop between neighboring sites at a rate of about 1 per minute at this temperature. From this a diffusion barrier between 0.4 and 0.5 eV can be inferred.

Upon exposure to H_2 the mobility of the isolated atoms increases noticeably, as shown in the images of Figure 2. These images are snapshots of a series of images acquired at 1 minute time intervals at a surface temperature of 144 K. The mobility of the O atoms is particularly visible in the continuous rearrangements in the lines of O atoms.

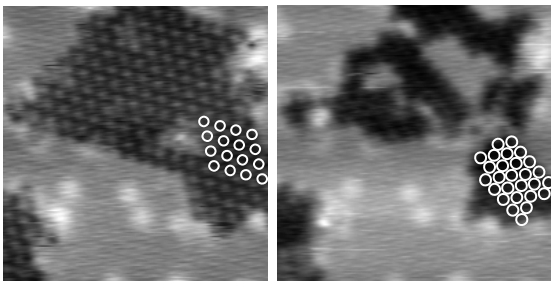

Figure 3. STM images (7.5×7.5 nm) obtained at 185K. Left panel: (2×2) oxygen islands. Right panel: After saturation of H, the islands compress into a (√3×√3)-O structure. Superimposed white circles on the O-atoms are shown. The process is reversible: after removal of the H the islands expand back to (2×2)-O.

Figure 3 shows an STM image (7.5×7.5 nm) obtained at 185 K showing oxygen islands with (2×2)-O structure. After saturation of the surface by exposure to H_2 (H atoms are invisible in the image under these conditions, due to weak contrast and high mobility), the islands compress into a (√3×√3)-O structure. The process is reversible: after removal of the H the islands expand back to (2×2)-O.

In separate experiments we have shown that H forms a (1×1) structure under similar exposure conditions, with vacancies that diffuse and aggregate to produce active sites for the dissociation of the incoming H_2 molecules [20,21].

3.2 Theoretical results

The unit cell is large enough to allow us to study the energy of different oxygen structures on the Pd(111) surface, up to (4×4)-O, with oxygen occupying three fold fcc hollow sites. Figure 1(b) illustrates the geometry of the (2×2)-O structure. The description of other structures considered here can be found elsewhere [32].

The stability of a phase can be conveniently described in terms of the formation energies of the clean and saturated surface as:

$$E_{form} = E_{sc} - (1-x)E_{Pd} - xE_{(1\times1)-O} \quad (1)$$

where, E_{sc}, E_{Pd}, and $E_{(1\times1)\text{-}O}$ are, respectively, the computed total energies of the supercell, bare Pd surface, and a fully oxygen (1×1) covered Pd surface, and x is the oxygen coverage. Below, we follow the structure notation of Ref. 32, where the phase diagram of oxygen adsorbed on platinum (111) surface was calculated from first principles.

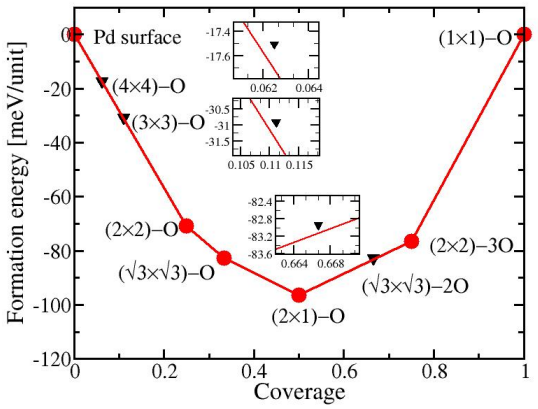

Figure 4. Formation energies of adsorbed oxygen phases on Pd(111). The lowest formation energies (circles) correspond to the stable phases. The triangles show formation energies of structures slightly above the lines connecting the stable phases (insets show blow-ups around these unstable phases).

Figure 4 shows the formation energies at various O coverages, computed for the phases selected as candidates for stable phases, similarly to the Pt(111)-oxygen phase diagram calculated previously using the cluster expansion method [32]. In the diagram of Figure 4, if the formation energy of a given phase is above the line connecting two

neighboring phases, this phase is unstable. As a result, the (4×4)-O, (3×3)-O, and (√3×√3)–2O phases are unstable. For all coverages *x* below 0.25 as in our experiments, stable phases occur only for zero and 0.25 coverage, which corresponds to a phase separation into (2×2)-O and bare Pd surface.

The same calculated data can be represented in the form of adsorption energies, as shown in Table I. The adsorption energy is defined as the difference between the total energy of the supercell and the energy of its constituents:

$$E_{ads} = \frac{1}{N_{at}}\left[E_{sc} - E_{Pd}\right] - E_O \qquad (2)$$

where, E_O is the computed total energy of an isolated oxygen atom, and N_{at} is the number of oxygen adsorbate atoms on the surface. A spin-polarized calculation is done for an isolated oxygen atom because in this case it has a substantial spin magnetic moment.

Table 1: Adsorption energies of the different possible structures of oxygen on the Pd(111) surface. The (2×2)-O and the O 2*a* lines are the lowest energy structures.

O structure on Pd(111)	E_{ads}, [eV/(O atom)]
(1×1)-O	-3.581
(2×2)–3O	-3.990
(√3×√3)–2O	-4.079
(2×1)-O	-4.352
(√3×√3)–O	-4.575
(2×2)-O	-4.715
(3×3)-O	-4.695
(4×4)-O	-4.702
√3*a* line	-4.689
2*a* line	-4.733

We find that the most stable geometry is the (2×2)-O, in agreement with the experimental results where (2×2)-O islands are observed to form with the STM before completion of 0.25 ML. We have also computed the energies of lines of oxygen atoms with 2*a* and √3*a* Pd-Pd spacings, observed experimentally (Figure 2).

While the structures corresponding to coverages over 1/3 have substantially higher energy than the rest, the energy of the (2×2)-O structure is only 13.1 meV/atom lower than that of the (4×4)-O, 20.4 meV/atom lower than (3×3)-O, and 140 meV/atom lower than (√3×√3)-O. Thus, there is a fine balance of repulsion and attraction between the oxygen atoms. Substrate mediated interactions are likely to be determined by Friedel oscillations, which are implicitly included in the DFT calculations.

Other interactions such as Van der Waals, can be estimated as empirical corrections to the DFT (following Reference [33]). We find that such contributions can be neglected due to their small values. For example for oxygen atoms separated by 5.59 Å, as in (2×2)-O structure, the Van der Waals energy is estimated to be 0.33 meV/atom.

Interestingly lines of O atoms with 2*a* Pd-Pd spacing have 18 meV/atom lower energy than the (2×2)-O islands, while the √3*a* O-lines have 44 meV/atom higher energy than the 2*a* lines, and 114 meV/atom lower energy than the (√3×√3)-O islands. These results are in good qualitative agreement with the experimental observations, shown in Figure 2. Since the differences in energies are close to *kT* it is kinetically difficult to form long straight O lines. When H atoms are co-adsorbed the 2*a* O-lines are transformed into shorter √3*a* O-lines. This is due to the increased O mobility (partly caused by H-O repulsion, discussed below), and to the pressure to reduce the length of the line and thus create more sites for H adsorption. Further increase of H adsorption converts all lines into the more compact (2×2)-O islands, overcoming the entropy effects. Finally, upon saturation of the surface with hydrogen, the (2×2)-O islands will be further compressed into (√3×√3)-O islands, reducing their area. More quantitative discussion of this process is presented later in this section.

The adsorption and electronic properties of hydrogen on Pd(111) have been studied by DFT methods in the past [34], showing stable

adsorption at hollow fcc sites, with hollow hcp site being less stable [35]. Here, the relaxed hydrogen to Pd atom distance is found to be 1.84 Å, which corresponds to a height of about 0.91 Å. This is in close agreement with previous studies [35].

To study the interaction of oxygen and hydrogen we fix the position of the hydrogen atom and move the oxygen atom along neighboring fcc hollow sites. The adsorption energy definition (Equation 2) is then modified by subtracting the energy of the Pd surface with a hydrogen atom E_{Pd+H}, rather than that of the bare Pd surface E_{Pd}. Figure 5(a) shows the geometry and the distances between the hydrogen and oxygen atoms in the fcc hollow sites, computed in the supercell described above. Figure 5(b) shows the adsorption energy as a function of the distance between oxygen and hydrogen for the five O - H separations shown in Figure 5(a). The system is more stable when H and O are farther apart, indicating repulsive interaction between H and O atoms at all distances. However, this repulsion is only appreciable when the distance between the atoms is that of the nearest fcc hollow cites, i.e. 2.97 Å. The atoms repulsive interaction is significantly smaller for separations exceeding 4.78 Å.

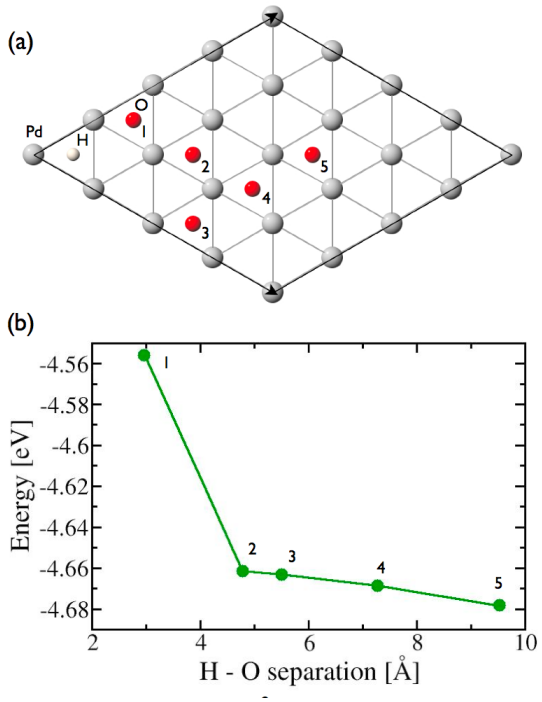

Figure 5: (a) Pd(111) plane and five O-H coadsorption geometries in the supercell used in this work, both atoms occupy their lowest energy fcc hollow sites. **(**b) Oxygen adsorption energy in the presence of hydrogen, for the five O-H separations shown in (a). The repulsive interaction between H and O atoms is practically negligible for separations exceeding the distance between second nearest fcc hollow sites (point 2).

This means that in order for the H atoms to compress the (2×2) oxygen island into the (√3×√3) oxygen island, the coverage of hydrogen atoms should be high enough to cover all the sites up to the edges of the oxygen island. We can estimate the energies required for such process based on adsorption energies. The (2×2)-O to (√3×√3)–O structure transformation energy (per oxygen atom) can be approximated as:

$$\Delta E = (E_{\sqrt{3}\times\sqrt{3}})/N_O - (E_{2\times 2})/N_O + \gamma(E_{H(1\times 1)})/N_H \qquad (3)$$

where, $E_{2\times 2}$ and $E_{\sqrt{3}\times\sqrt{3}}$ are the oxygen adsorption energies in the (2×2)-O and (√3×√3)-O phases respectively, $E_{H(1\times 1)}$ is the hydrogen adsorption energy in the (1×1) phase, and γ is a factor near unity corresponding to the assumption that the area ΔA, freed by the oxygen compression from (2×2)-O to (√3×√3)-O, is be filled by H:

$$\Delta A/N_O = \gamma \Delta A/N_H . \qquad (4)$$

Here, N_O and N_H are the numbers of oxygen and hydrogen atoms filling the area ΔA. The experimental adsorption energy (from the measured adsorption heat) for hydrogen on Pd(111) is 0.902 eV/(H atom), which was found to be very weakly dependent on temperature and ambient pressure [12]. By contrast the theoretical calculations within the GGA approximation gives a hydrogen adsorption energy of 0.59 eV/(H atom) [36]. Using this conservative value, and ignoring island edge effects, we can conclude the following. From our calculations (Table I) the energy required to convert a (2×2)-O island into a (√3×√3)-O island is +0.14 eV/(O atom).

At the same time, the adsorption energy due to the coadsorbed hydrogen is -0.59 eV/(H atom). The area unit factor in this case is very close to unity, i.e. 0.9985, therefore leading to the structure transformation energy ΔE, (per O atom) of -0.45 eV. Since the overall energy balance is negative, the energy released due to the coadsorption of hydrogen is sufficient for such transformation to occur. At the same time, the energy required to transform a (2×2)-O island into a (1×1)-O island is estimated from our calculations to be +1.13 eV/(O atom). This leads to the transformation energy ΔE of +0.54 eV/(O atom). The coadsorption of hydrogen in this case would not release enough energy for the transformation to occur. Thus, such a transformation is not feasible from our calculations, and it is not observed experimentally. The energy required to transform a line from the (2×2)-O into ($\sqrt{3}\times\sqrt{3}$)-O geometry is significantly lower, i.e. +0.044 eV/(O atom), which is illustrated in experiment by the earlier transition of lines in comparison with islands.

We now turn to study the effect of H on the mobility of O. For that we consider several stable positions of O as a function of its distance from a hydrogen atom, taking into account the results shown in Figure 5. These positions are shown in Figure 6(a). Two fcc sites close to the H atom labeled S_1 and S_2, are situated 2.75 Å and 5.5 Å away, respectively. The actual O-H distance when O and H atom occupy these sites is 2.967 Å and 5.501 Å, due to the vertical relaxation of O and H atoms with respect to each other. In this section any position farther than the third fcc hollow site (8.25 Å away from H atom) is considered an isolated site (labeled S_i), due to its weak interaction with hydrogen. In addition to the fcc sites, there are hollow hcp cites (labeled S_h), which are local energy minima for the O atoms.

The energy barrier heights between these sites are the key parameters to study the mobility of oxygen along the Pd(111) surface. Following previous DFT studies of hydrogen on a Pd(111) surface [35], we consider the bridge sites as the energy barriers between fcc and hcp sites. In Figure 6(a) we show a possible path and barriers for diffusion of oxygen, along the direction indicated by the arrow, starting with S_1. The O atom at (S_1) can move either through (B_1) to a position very close to H, or through (B_2) to an hcp site (S_h). Here we are computing the changes in barrier heights when O moves away from the H. The next jump over the bridge site (B_3) leads to an fcc hollow site (S_2). Further, moving over the bridge (B_4) leading to another hcp site an oxygen atom reaches an isolated site (S_i) where its interaction with H can be considered negligible.

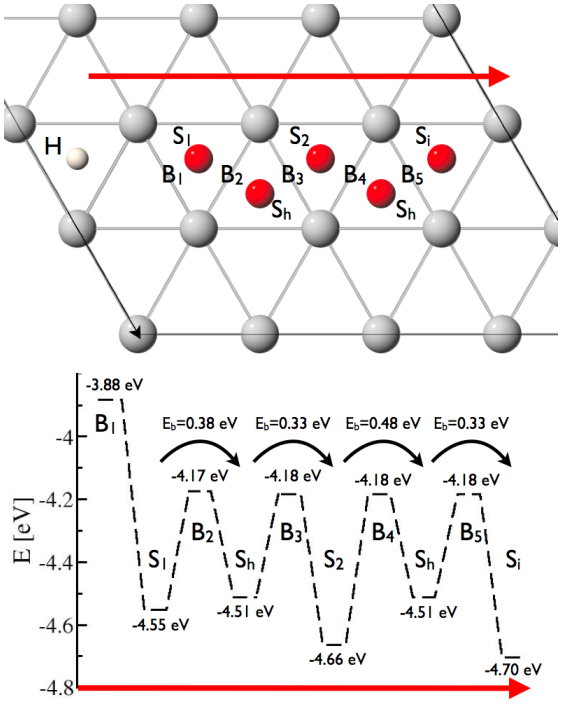

Figure 6: a) Schematic diagram showing the relevant hollow and bridge sites along the diffusion path of an O atom on the Pd(111) surface. The O atom hops over a series of barriers between fcc and hcp hollow sites, where the energy has a local minimum. b) Local energy minima and barrier heights for the O atom following the path indicated by the arrow in (a).

In Figure 6(b) we show the resulting local energy minima and barriers encountered by an O atom diffusing from S_1 to S_i. With the exception of the bridge site in the immediate vicinity of the H, the energies of oxygen atoms at the bridge sites are practically the same, -4.18 eV. This indicates that the diffusion barrier is determined by the energies of the adjacent minima at fcc and hcp hollow sites. As in Figure 5(b) the energy of the O atom in fcc sites decreases as it moves farther away

from the H atom, from -4.55 to -4.70 eV. The hcp hollow sites are predictably less stable, with oxygen energies of -4.51 eV. It is the destabilization of the energy of O at the S_1 site that reduces the energy barrier for the jump from S_1 to S_h by a considerable 0.15 eV (per Oxygen atom), as compared for the energy barrier in the absence of H, i.e., from S_i to S_h. This explains the observed increase of the mobility of oxygen when hydrogen is coadsorbed on the Pd(111) surface.

The increase in diffusivity is expected to occur at short range, when H covers most of the free Pd(111) surface, thereby approaching the O atoms. The O atoms would then be forced to modify their surface structure with neighboring fcc hollow sites. This, in addition to the finding that (4×4)-O and (3×3)-O structures have slightly higher energies in comparison with (2×2)-O structure, suggests that the presence of hydrogen on the Pd(111) surface should compress the oxygen islands into the denser (√3×√3)-O structure, rather than dissolve them into (4×4)-O or a looser structure. This is indeed what the experiments show.

Another manifestation of the repulsive adsorbate interactions described above is that the water formation reaction does not occur, until the pressure and temperature are increased beyond 220 K and 10^{-7} Torr [21, 23].

CONCLUSIONS

The interaction between O and H on Pd(111) has been studied in detail, both theoretically using DFT calculations and experimentally with STM microscopy. The results indicate that the total energy differences between the various O island structures can account for the experimentally observed (2×2)-O structure and the formation of lines of O atoms with 2*a* and √3*a* atomic spacing. We have shown how in the presence of hydrogen the repulsive interaction between O and H atoms is responsible for the observed (2×2)-O to (√3×√3)-O structural transition. The energy released due to the adsorption of hydrogen being sufficient to drive such structure change.

We have also shown that the repulsion between H and O and the increasing of the oxygen mobility are closely related. The reduction of the barrier heights from first to second fcc hollow neighboring sites due to the repulsion between atoms increases the mobility of oxygen. At the same time these energy barriers increase back to their isolated atom values beyond the second fcc hollow neighbor sites, which indicates that the effect is short ranged. The repulsive interaction between O and H at short range also explains why in order to for the water formation reaction to occur high temperature and coverage of H is needed.

ACKNOWLEDGMENTS

This work was supported by the Director, Office of Science, Office of Basic Energy Sciences, Materials Sciences and Engineering Division, of the U.S. Department of Energy under Contract No. DE-AC02-05CH11231, and by the National Energy Research Scientific Computing Center (NERSC).

[1] H. Over, Prog. Surf. Sci. 58 (1998) 249.
[2] T. Engle, H. Kuipers, Surf. Sci. 90 (1979) 181.
[3] S. Völkening, K. Bedürftig, K. Jacobi, J. Wintterlin, G. Ertl, Phys. Rev. Lett. 83 (1999) 2672.
[4] K. Bedürftig, S. Völkening, Y. Wang, J. Wintterlin, K. Jacobi, G. Ertl, J. Chem. Phys. 111 (1999) 11147.
[5] M. Schick, J. Xie, W.J. Michell, W.H. Weinberg, J. Chem. Phys. 104 (1996) 7713.
[6] S. Ljungström, B. Kasemo, A. Rosen, T. Wahnström, E. Fridell, Surf. Sci. 216 (1989) 63.
[7] A. de Meijere, K.W. Kolasinski, E. Hasselbrink, Faraday Discuss. 96 (1993) 265.
[8] K.D. Gibson, J.I. Colonell, S.J. Sibener, Faraday Discuss. 103 (1995) 6735.
[9] S. Wilke, V. Natoli, M.H. Cohen, J. Chem. Phys. 112 (2000) 9986.
[10] M. K. Rose, A. Borg, J. C. Dunphy, T. Mitsui, D. F. Ogletree, and M. Salmeron, Surf. Sci. 547 (2003) 162.
[11] M. K. Rose, A. Borg, J. C. Dunphy, T. Mitsui, D. F. Ogletree, and M. Salmeron, Surf. Sci. 561 (2004) 69.
[12] H. Conrad, G. Ertl and E. E. Latta, Surf. Sci. 41 (1974) 435.
[13] S. G. Louie, Phys. Rev. Lett. 42 (1979) 476.
[14] T.E. Felter, S.M. Foiles, M.S. Daw, R.H. Stulen, Surf. Sci. 171 (1986) L379.
[15] A.P. Seitsonen, Y.D. Kim, S. Schwegmann, H. Over, Surf. Sci. 468 (2000) 176.
[16] T.E. Felter, E.C. Sowa, M.A. Van Hove, Phys. Rev. B 40 (1989) 891.
[17] R.J. Behm, V. Penka, M.-G. Cattania, K. Christmann, G. Ertl, J. Chem. Phys. 78 (1983) 7486.
[18] M.S. Daw, S.M. Foiles, Phys. Rev. B 35 (1987) 2128.
[19] O.M. Løvvik, R.A. Olsen, Phys. Rev. B 58 (1998) 10890.
[20] T. Mitsui, M. K. Rose, E. Fomin, D. F. Ogletree, and M. Salmeron, Nature 422 (2003) 705.
[21] T. Mitsui, M. K. Rose, E. Fomin, D. F. Ogletree, and M. Salmeron, Surf.Sci. 540 (2003) 5.
[22] H. Conrad, G. Ertl, J. Küppers, Surf. Sci. 76 (1978) 323.
[23] T. Mitsui, M. K. Rose, E. Fomin, D. F. Ogletree, and M. Salmeron, Surf.Sci. 511 (2002) 259.
[24] G. Kresse and J. Hafner, Phys. Rev. B 49 (1994) 14251.
[25] G. Kresse and J. Furthmuller, Comput. Mater. Sci. 6 (1996) 15.
[26] Y. Wang and J. P. Perdew, Phys. Rev. B 44 (1991) 13298.
[27] J. P. Perdew, K. Burke, and M. Ernzerhof, Phys. Rev. Lett. 77 (1996) 3865.
[28] Y. Zhang, V. Blum, and K. Reuter, Phys. Rev. B 75, 235406 (2007).
[29] P. Pulay, Chem. Phys. Lett. 73 (1980) 393.
[30] J. M. Blanco, C. González, P. Jelínek, J. Ortega, F. Flores, R. Pérez, M. Rose, M. Salmeron, J. Méndez, J.Wintterlin, and G. Ertl, Phys. Rev. B 71 (2005) 113402.
[31] M. K. Rose, T. Mitsui, A. Borg, D. F. Ogletree, and M. Salmeron, J Chem. Phys. 115 (2001) 10927.
[32] H. Tang, A. Van der Ven, and B. L. Trout, Phys. Rev. B 70, 045420 (2004).
[33] W. T. M. Mooij, F. B. van Duijneveldt, J. G. C. M. van Duijneveldt-van de Rijdt, and B. P. van Eijck, J. Phys. Chem. A 103 (1999) 9872.
[34] M. Todorova, K. Reuter, and M. Scheffler, J. Phys. Chem. B 108, 14477 (2004).
[35] J. F. Paul, P. Sautet, Phys. Rev. B 53 (1996) 8015.
[36] C. Morin, D. Simon, P. Sautet, Surf. Sci. 600 (2006) 1339.